

Chapter 4

Frequency Correction

Dariusz Divsalar

Over the years, much effort has been spent in the search for optimum synchronization schemes that are robust and simple to implement [1,2]. These schemes were derived based on maximum-likelihood (ML) estimation theory. In many cases, the derived open- or closed-loop synchronizers are nonlinear. Linear approximation provides a useful tool for the prediction of synchronizer performance.

In this semi-tutorial chapter, we elaborate on these schemes for frequency acquisition and tracking. Various low-complexity frequency estimator schemes are presented in this chapter. The theory of ML estimation provides the optimum schemes for frequency estimation. However, the derived ML-based scheme might be too complex for implementation. One approach is to use theory to derive the best scheme and then try to reduce the complexity such that the loss in performance remains small. Organization of this chapter is as follows: In Section 4.1, we show the derivation of open- and closed-loop frequency estimators when a pilot (residual) carrier is available. In Section 4.2, frequency estimators are derived for known data-modulated signals (data-aided estimation). In Section 4.3, non-data-aided frequency estimators are discussed. This refers to the frequency estimators when the data are unknown at the receiver.

4.1 Frequency Correction for Residual Carrier

Consider a residual-carrier system where a carrier (pilot) is available for tracking. We consider both additive white Gaussian noise (AWGN) and Rayleigh fading channels in this section.

4.1.1 Channel Model

Let $\tilde{r}_c[k]$ be the k th received complex sample of the output of a low-pass filtered pilot. The observation vector $\tilde{\mathbf{r}}_c$ with components $\tilde{r}_c[k]$; $k = 0, 1, \dots, N - 1$ can be modeled as

$$\tilde{r}_c[k] = Ae^{j(2\pi\Delta f k T_s + \theta_c)} + \tilde{n}[k] \quad (4-1)$$

where the $\tilde{r}_c[k]$ samples are taken every T_s seconds (sampling rate of $1/T_s$). In the above equation, $\tilde{n}[k]$, $k = 0, 1, \dots, N - 1$, are independent, identically distributed (iid) zero-mean, complex Gaussian random variables with variance σ^2 per dimension. The frequency offset to be estimated is denoted by Δf , and θ_c is an unknown initial carrier phase shift that is assumed to be uniformly distributed in the interval $[0, 2\pi)$ but constant over the N samples. For an AWGN channel, $A = \sqrt{2P_c}$ is constant and represents the amplitude of the pilot samples. For a Rayleigh fading channel, we assume A is a complex Gaussian random variable, where $|A|$ is Rayleigh distributed and $\arg A \triangleq \tan^{-1}(\text{Im}(A)/\text{Re}(A))$ is uniformly distributed in the interval $[0, 2\pi)$, where $\text{Im}(\cdot)$ denotes the imaginary operator and $\text{Re}(\cdot)$ denotes the real operator.

4.1.2 Optimum Frequency Estimation over an AWGN Channel

We desire an estimate of the frequency offset Δf based on the received observations given by Eq. (4-1). The ML estimation approach is to obtain the conditional probability density function (pdf) of the observations, given the frequency offset. To do so, first we obtain the following conditional pdf:

$$P(\tilde{\mathbf{r}}_c | \Delta f, \theta_c) = C_0 e^{-(1/2\sigma^2)Z} \quad (4-2)$$

where C_0 is a constant, and

$$Z = \sum_{k=0}^{N-1} \left| \tilde{r}_c[k] - Ae^{j(2\pi\Delta f k T_s + \theta_c)} \right|^2 \quad (4-3)$$

Define

$$Y = \sum_{k=0}^{N-1} \tilde{r}_c[k] e^{-j(2\pi\Delta f k T_s)} \quad (4-4)$$

Then Z can be rewritten as

$$Z = \sum_{k=0}^{N-1} |\tilde{r}_c[k]|^2 - 2A\text{Re}(Ye^{-j\theta_c}) + \sum_{k=0}^{N-1} A^2 \quad (4-5)$$

The first and the last terms in Eq. (4-5) do not depend on Δf and θ_c . Denoting the sum of these two terms by C_1 , then Z can be written as

$$Z = C_1 - 2A|Y|\cos(\theta_c - \arg Y) \quad (4-6)$$

Using Eq. (4-6), the conditional pdf of Eq. (4-2) can be written as

$$P(\tilde{\mathbf{r}}_c|\Delta f, \theta_c) = C_2 \exp \left[\frac{A}{\sigma^2} |Y|\cos(\theta_c - \arg Y) \right] \quad (4-7)$$

where $C_2 = Ce^{-(C_1/2\sigma^2)}$. Averaging Eq. (4-7) over θ_c produces

$$P(\tilde{\mathbf{r}}_c|\Delta f) = C_2 I_0 \left(\frac{A|Y|}{\sigma^2} \right) \quad (4-8)$$

where $I_0(\cdot)$ is the modified Bessel function of zero order and can be represented as

$$I_0(x) = \frac{1}{2\pi} \int_0^{2\pi} e^{x\cos(\psi)} d\psi \quad (4-9)$$

Since $I_0(x)$ is an even convex \cup function of x , maximizing the right-hand side of Eq. (4-8) is equivalent to maximizing $|Y|$. Thus, the ML metric for estimating the frequency offset can be obtained by maximizing the following metric:

$$\lambda(\Delta f) = |Y| = \left| \sum_{k=0}^{N-1} \tilde{r}_c[k] e^{-j(2\pi\Delta f k T_s)} \right| \quad (4-10)$$

4.1.3 Optimum Frequency Estimation over a Rayleigh Fading Channel

We desire an estimate of the frequency offset Δf over a Rayleigh fading channel. The ML approach is to obtain the conditional pdf of the observations,

given the frequency offset. To do so, first we start with the following conditional pdf:

$$P(\tilde{\mathbf{r}}_{\mathbf{c}}|A, \Delta f, \theta_c) = C_0 e^{-(1/2\sigma^2)Z} \quad (4-11)$$

where C_0 is a constant, and Z and Y are defined as in Eqs. (4-3) and (4-4). Since A is now a complex random variable, then Z can be rewritten as

$$Z = \sum_{k=0}^{N-1} |\tilde{r}_c[k]|^2 - 2\text{Re}(Y A e^{-j\theta_c}) + \sum_{k=0}^{N-1} |A|^2 \quad (4-12)$$

The first terms in Eq. (4-12) do not depend on A . Averaging the conditional pdf in Eq. (4-11) over A , assuming the magnitude of A is Rayleigh distributed and its phase is uniformly distributed, we obtain

$$P(\tilde{\mathbf{r}}_{\mathbf{c}}|\Delta f, \theta_c) = C_3 \exp\left(\frac{C_4}{2\sigma^2}|Y|^2\right) \quad (4-13)$$

where C_3 and C_4 are constants, and Eq. (4-13) is independent of θ_c . Thus, maximizing the right-hand side of Eq. (4-13) is equivalent to maximizing $|Y|^2$ or equivalently $|Y|$. Thus, the ML metric for estimating the frequency offset can be obtained by maximizing the following metric:

$$\lambda(\Delta f) = |Y| = \left| \sum_{k=0}^{N-1} \tilde{r}_c[k] e^{-j(2\pi\Delta f k T_s)} \right| \quad (4-14)$$

which is identical to that obtained for the AWGN channel case.

4.1.4 Open-Loop Frequency Estimation

For an open-loop estimation, we have

$$\widehat{\Delta f} = \underset{\Delta f}{\text{argmax}} \lambda(\Delta f) \quad (4-15)$$

However, this operation is equivalent to obtaining the fast Fourier transform (FFT) of the received sequence, taking its magnitude, and then finding the maximum value, as shown in Fig. 4-1.

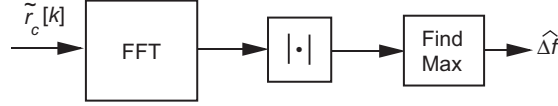


Fig. 4-1. Open-loop frequency estimation, residual carrier.

4.1.5 Closed-Loop Frequency Estimation

The error signal for a closed-loop estimator can be obtained as

$$e = \frac{\partial}{\partial \Delta f} \lambda(\Delta f) \quad (4-16)$$

We can approximate the derivative of $\lambda(\Delta f)$ for small ε as

$$\frac{\partial}{\partial \Delta f} \lambda(\Delta f) = \frac{\lambda(\Delta f + \varepsilon) - \lambda(\Delta f - \varepsilon)}{2\varepsilon} \quad (4-17)$$

Then, we can write the error signal as (in the following, any positive constant multiplier in the error signal representation will be ignored)

$$e = |Y(\Delta f + \varepsilon)| - |Y(\Delta f - \varepsilon)| \quad (4-18)$$

where

$$Y(\Delta f + \varepsilon) = \sum_{k=0}^{N-1} \tilde{r}_c[k] e^{-j(2\pi\Delta f k T_s)} e^{-j(2\pi\varepsilon k T_s)} \quad (4-19)$$

The error-signal detector for a closed-loop frequency correction can be implemented based on the above equations. The block diagram is shown in Fig. 4-2, where in the figure $\alpha = e^{-j2\pi\varepsilon T_s}$.

Now rather than using the approximate derivative of $\lambda(\Delta f)$, we can take the actual derivative of $\lambda^2(\Delta f) = |Y|^2$, which gives the error signal

$$e = \text{Im}(Y^*U) \quad (4-20)$$

where

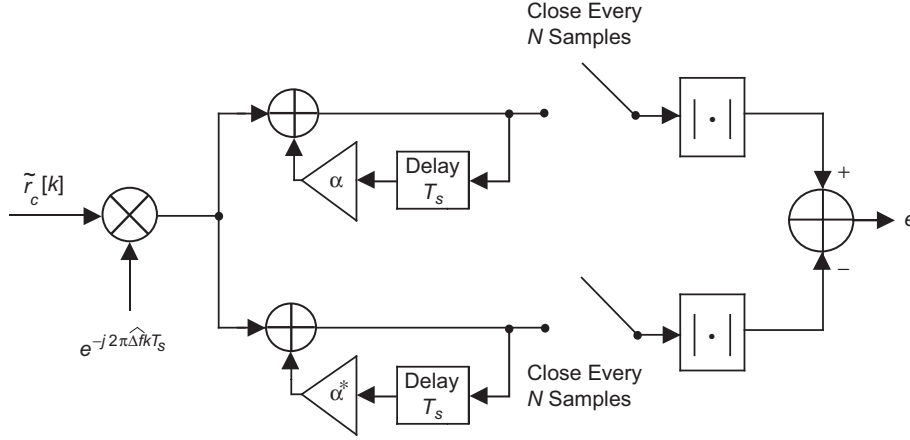


Fig. 4-2. Approximate error signal detector, residual carrier.

$$U = \sum_{k=0}^{N-1} \tilde{r}_c[k] k e^{-j(2\pi\Delta f k T_s)} \quad (4-21)$$

Note that the error signal in Eq. (4-20) can also be written as

$$e = \text{Im}(Y^*U) = |Y - jU|^2 - |Y + jU|^2 \quad (4-22)$$

or for a simple implementation we can use

$$e = |Y - jU| - |Y + jU| \quad (4-23)$$

The block diagram of the error signal detector based on Eq. (4-23) is shown in Fig. 4-3.

The corresponding closed-loop frequency estimator is shown in Fig. 4-4. The dashed box in this figure and all other figures represents the fact that the hard limiter is optional. This means that the closed-loop estimators can be implemented either with or without such a box.

4.1.5.1. Approximation to the Optimum Error Signal Detector. Implementation of the optimum error signal detector is a little bit complex. To reduce the complexity, we note that

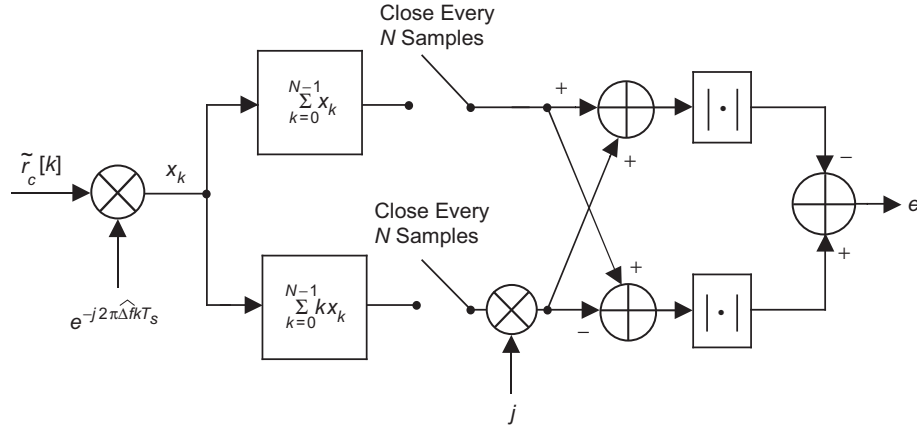


Fig. 4-3. Exact error signal detector, residual carrier.

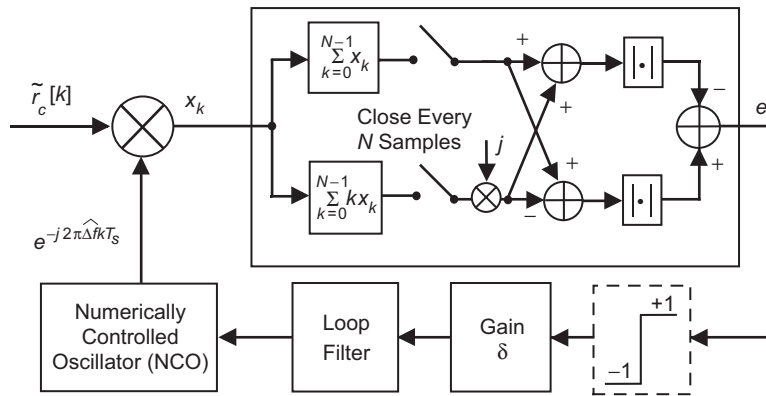


Fig. 4-4. Closed-loop frequency estimator, residual carrier.

$$e = \text{Im}(Y^*U) = \sum_{i=0}^{N-1} \text{Im}(X_{0,i}^* X_{i+1,(N-1)}) \cong C_5 \text{Im}(X_{0,(N/2)-1}^* X_{(N/2),N-1}) \quad (4-24)$$

where

$$X_{m,n} = \sum_{k=m}^n \tilde{r}_c[k] e^{-j(2\pi\Delta f k T_s)} \quad (4-25)$$

The closed-loop frequency estimator with the approximate error signal detector given by Eq. (4-24) is shown in Fig. 4-5. The parameters $N_w = N/2$ (the

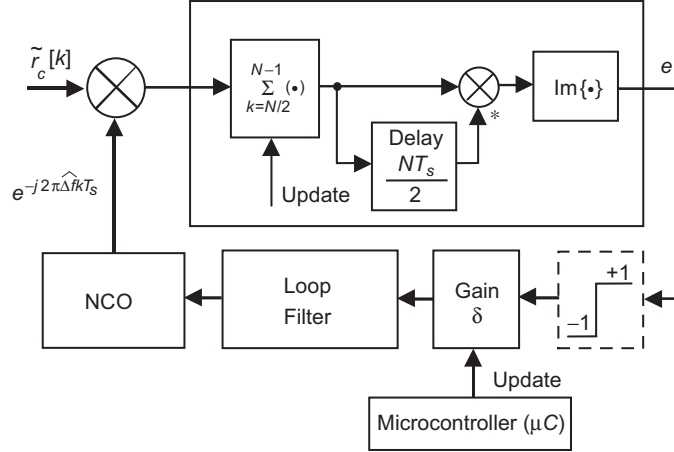


Fig. 4-5. Low-complexity closed-loop frequency correction, residual carrier.

number of samples to be summed, i.e., the window size) and δ (gain) should be optimized and updated after the initial start to perform both the acquisition and tracking of the offset frequency.

4.1.5.2. Digital Loop Filter. The gain δ that was shown in the closed-loop frequency-tracking system is usually part of the digital loop filter. However, here we separate them. Then the digital loop filter without gain δ can be represented as

$$F(z) = 1 + \frac{b}{1 - z^{-1}} \quad (4-26)$$

The corresponding circuit for the digital loop filter is shown in Fig. 4-6. Now in addition to the gain δ , the parameter b also should be optimized to achieve the best performance.

4.1.5.3. Simulation Results. Performance of the closed-loop frequency estimator in Fig. 4-5 was obtained through simulations. First, the acquisition of the closed-loop estimator for a 10-kHz frequency offset is shown in Fig. 4-7. Next the standard deviation of the frequency error versus the received signal-to-noise ratio (SNR) for various initial frequency offsets was obtained. The results of the simulation are shown in Fig. 4-8.

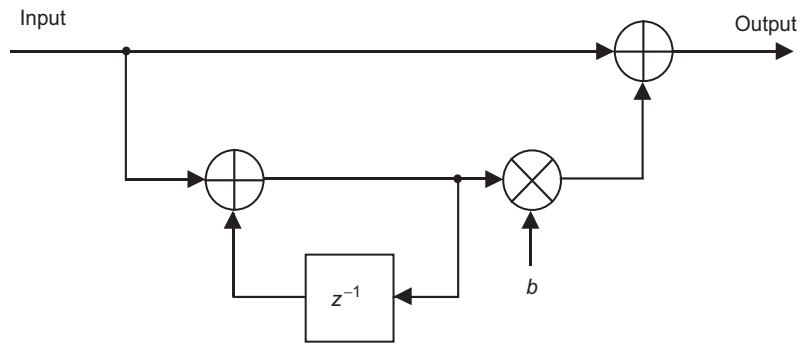


Fig. 4-6. Loop filter for frequency-tracking loops.

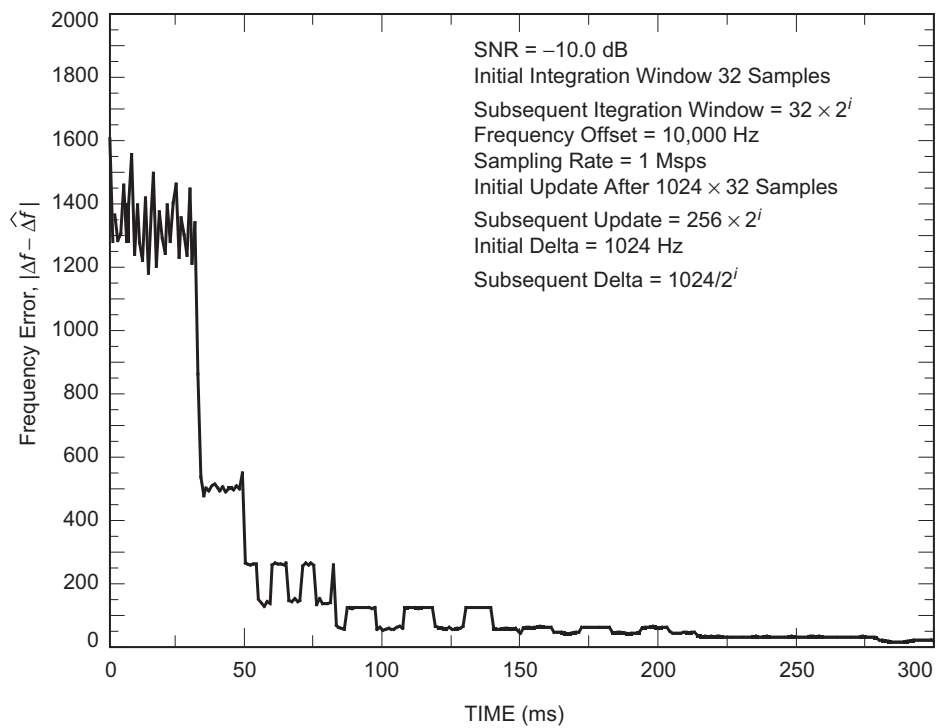


Fig. 4-7. Frequency acquisition performance.

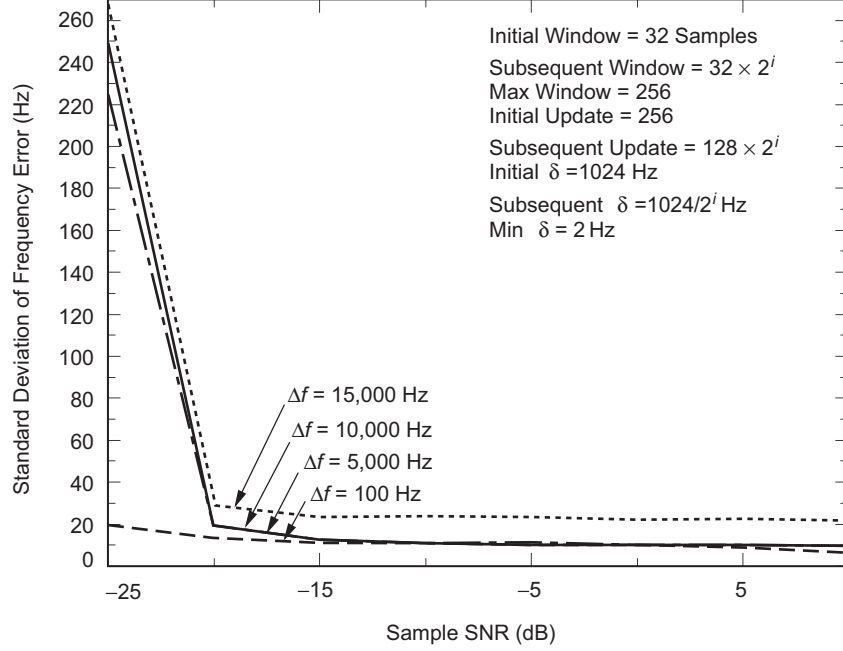


Fig. 4-8. Standard deviation of frequency error.

4.2 Frequency Correction for Known Data-Modulated Signals

Consider a data-modulated signal with no residual (suppressed) carrier. In this section, we assume perfect knowledge of the symbol timing and data (data-aided system). Using again the ML estimation, we derive the open- and closed-loop frequency estimators.

4.2.1. Channel Model

We start with the received baseband analog signal and then derive the discrete-time version of the estimators. Let $\tilde{r}(t)$ be the received complex waveform, and a_i be the complex data representing an M -ary phase-shift keying (M -PSK) modulation or a quadrature amplitude modulation (QAM). Let $p(t)$ be the transmit pulse shaping. Then the received signal can be modeled as

$$\tilde{r}(t) = \sum_{i=-\infty}^{\infty} a_i p(t - iT) e^{j(2\pi\Delta f t + \theta_c)} + \tilde{n}(t) \quad (4-27)$$

where T is the data symbol duration and $\tilde{n}(t)$ is the complex AWGN with two-sided power spectral density N_0 W/Hz per dimension. The conditional pdf of the received observation given the frequency offset Δf and the unknown carrier phase shift θ_c can be written as

$$p(\tilde{\mathbf{r}}|\Delta f, \theta_c) = C_6 e^{-(1/N_0) \int_{-\infty}^{\infty} |\tilde{r}(t) - \sum_{i=-\infty}^{\infty} a_i p(t-iT) e^{j(2\pi\Delta f t + \theta_c)}|^2 dt} \quad (4-28)$$

where C_6 is a constant. Note that

$$\begin{aligned} \left| \tilde{r}(t) - \sum_{i=-\infty}^{\infty} a_i p(t-iT) e^{j(2\pi\Delta f t + \theta_c)} \right|^2 &= |\tilde{r}(t)|^2 + \left| \sum_{i=-\infty}^{\infty} a_i p(t-iT) \right|^2 \\ &\quad - 2 \sum_{i=-\infty}^{\infty} \operatorname{Re} \left\{ a_i^* \tilde{r}(t) p(t-iT) e^{-j(2\pi\Delta f t + \theta_c)} \right\} \end{aligned} \quad (4-29)$$

The first two terms do not depend on Δf and θ_c . Then we have

$$p(\tilde{\mathbf{r}}|\Delta f, \theta_c) = C_7 e^{(2/N_0) \operatorname{Re} \left\{ \sum_{i=-\infty}^{\infty} a_i^* z_i(\Delta f) e^{-j\theta_c} \right\}} \quad (4-30)$$

where C_7 is a constant and

$$z_i(\Delta f) = \int_{iT}^{(i+1)T} \tilde{r}(t) p(t-iT) e^{-j(2\pi\Delta f t)} dt \quad (4-31)$$

The conditional pdf in Eq. (4-30) also can be written as

$$p(\tilde{\mathbf{r}}|\Delta f, \theta_c) = C_7 \exp \left[\frac{2}{N_0} |Y| \cos(\theta_c - \arg Y) \right] \quad (4-32)$$

where

$$Y = \sum_{i=-\infty}^{\infty} a_i^* z_i(\Delta f) \quad (4-33)$$

Averaging Eq. (4-32) over θ_c produces

$$P(\tilde{\mathbf{r}}|\Delta f) = C_8 I_0 \left(\frac{2}{N_0} |Y| \right) \quad (4-34)$$

where C_8 is a constant. Again, since $I_0(x)$ is an even convex cup \cup function of x , maximizing the right-hand side of Eq. (4-34) is equivalent to maximizing $|Y|$ or equivalently $|Y|^2$. Thus, the ML metric for estimating the frequency offset over the N data symbol interval can be obtained by maximizing the following metric:

$$\lambda(\Delta f) = |Y| = \left| \sum_{k=0}^{N-1} a_k^* z_k(\Delta f) \right| \quad (4-35)$$

4.2.2 Open-Loop Frequency Estimation

For an open-loop estimation, we have

$$\widehat{\Delta f} = \underset{\Delta f}{\operatorname{argmax}} \lambda(\Delta f) \quad (4-36)$$

but this operation is equivalent to multiplying the received signal by $e^{-j(2\pi\Delta f t)}$, passing it through the matched filter (MF) with impulse response $p(-t)$, and sampling the result at $t = (k+1)T$, which produces the sequence of z_k 's. Next, sum the z_k 's, take its magnitude, and then find the maximum value by varying the frequency Δf between $-\Delta f_{max}$ and Δf_{max} , where Δf_{max} is the maximum expected frequency offset. The block diagram to perform these operations is shown in Fig. 4-9.

4.2.3 Closed-Loop Frequency Estimation

The error signal for closed-loop tracking can be obtained as

$$e = \frac{\partial}{\partial \Delta f} \lambda(\Delta f) \quad (4-37)$$

We can approximate the derivative of $\lambda(\Delta f)$ for small ε as in Eq. (4-17). Then we can approximate the error signal as

$$e = |Y(\Delta f + \varepsilon)| - |Y(\Delta f - \varepsilon)| \quad (4-38)$$

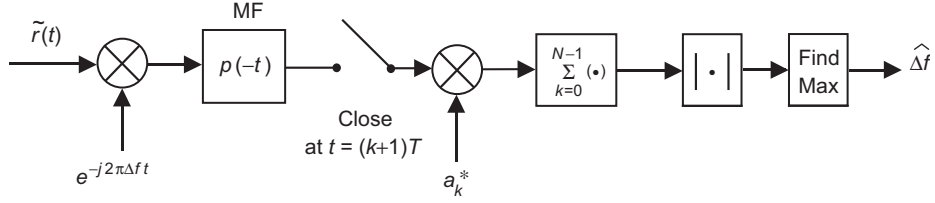


Fig. 4-9. Open-loop frequency estimation for suppressed carrier, known data.

where

$$Y(\Delta f + \varepsilon) = \sum_{k=0}^{N-1} a_k^* z_k(\Delta f + \varepsilon) \quad (4-39)$$

The error signal detector for the closed-loop frequency correction is implemented using the above equations and is shown in Fig. 4-10. In the figure, DAC denotes digital-to-analog converter.

Now again, rather than using the approximate derivative of $\lambda(\Delta f)$, we can take the derivative of $\lambda^2(\Delta f) = |Y|^2$ to obtain the error signal as

$$e = \text{Im}(Y^*U) \quad (4-40)$$

and

$$U = \sum_{k=0}^{N-1} a_k^* u_k(\Delta f) \quad (4-41)$$

where

$$u_i(\Delta f) = \int_{iT}^{(i+1)T} \tilde{r}(t) t p(t - iT) e^{-j(2\pi\Delta f t)} dt \quad (4-42)$$

Thus, $u_k(\Delta f)$ is produced by multiplying $\tilde{r}(t)$ by $e^{-j2\pi\Delta f t}$ and then passing it through a so-called derivative matched filter (DMF)—also called a frequency-matched filter (FMF)—with impulse response $tp(-t)$, and finally sampling the result of this operation at $t = (k + 1)T$. Note that the error signal in Eq. (4-40) also can be written as

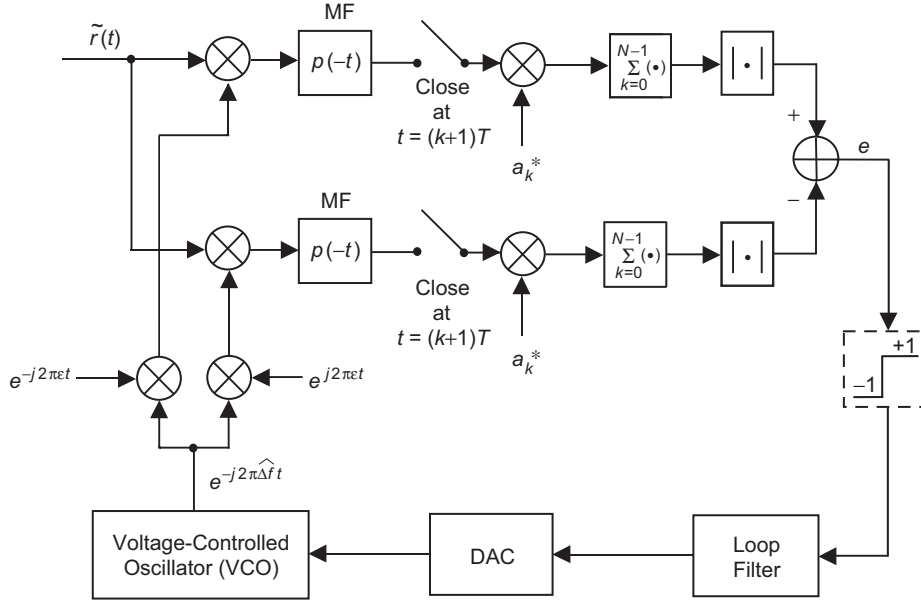


Fig. 4-10. Error signal detector and closed-loop block diagram for suppressed carrier, known data.

$$e = \text{Im}(Y^*U) = |Y - jU|^2 - |Y + jU|^2 \quad (4-43)$$

or, simply, we can use

$$e = |Y - jU| - |Y + jU| \quad (4-44)$$

The block diagram of the closed-loop frequency estimator using the error signal detector given by Eq. (4-40) is shown in Fig. 4-11. Similarly, the block diagram of the closed-loop frequency estimator using the error signal detector given by Eq. (4-44) is shown in Fig. 4-12.

The closed-loop frequency estimator block diagrams shown in this section contain mixed analog and digital circuits. An all-digital version of the closed-loop frequency estimator in Fig. 4-11 operating on the received samples $\tilde{r}[k]$ is shown in Fig. 4-13. In the figure, p_k represents the discrete-time version of the pulse shaping $p(t)$. We assume that there are n samples per data symbol duration T . An all-digital version of other closed-loop estimators can be obtained similarly.

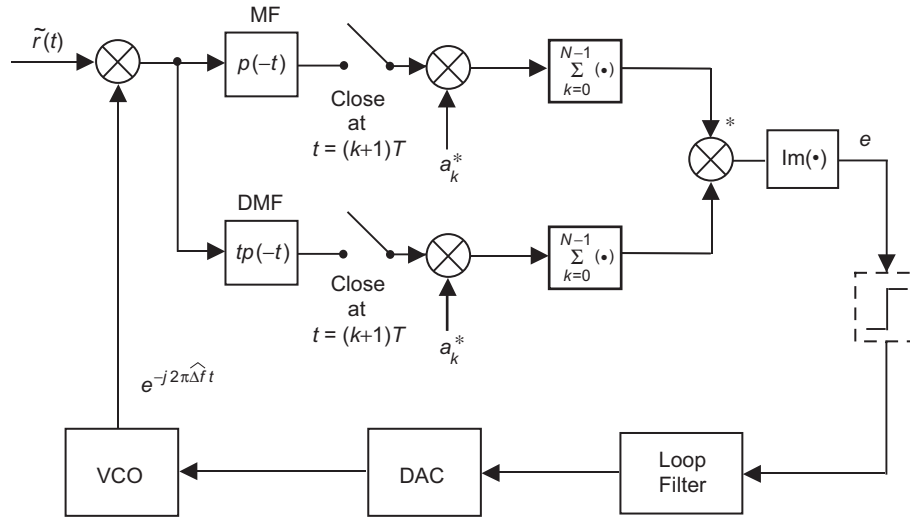


Fig. 4-11. Closed-loop estimator with error signal detector for suppressed carrier, known data, Eq. (4-40).

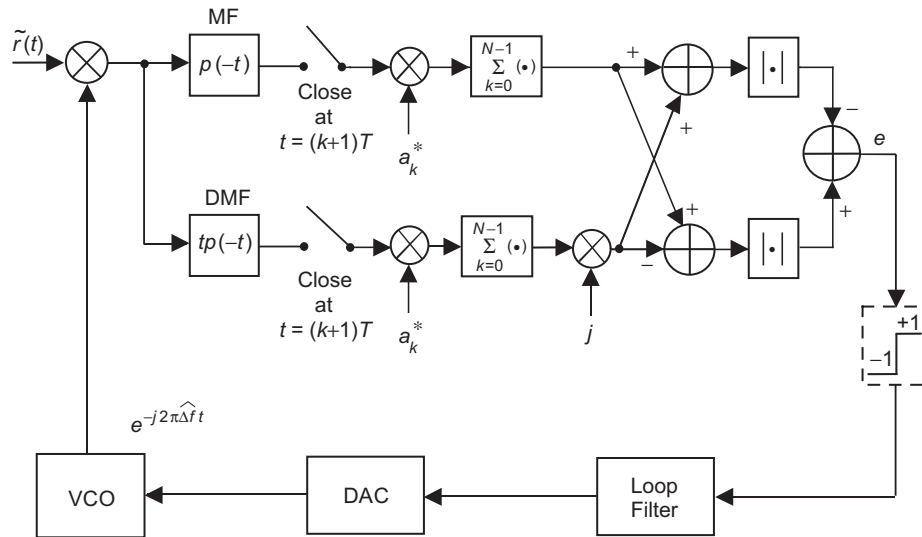


Fig. 4-12. Closed-loop estimator with error signal detector for suppressed carrier, known data, Eq. (4-44).

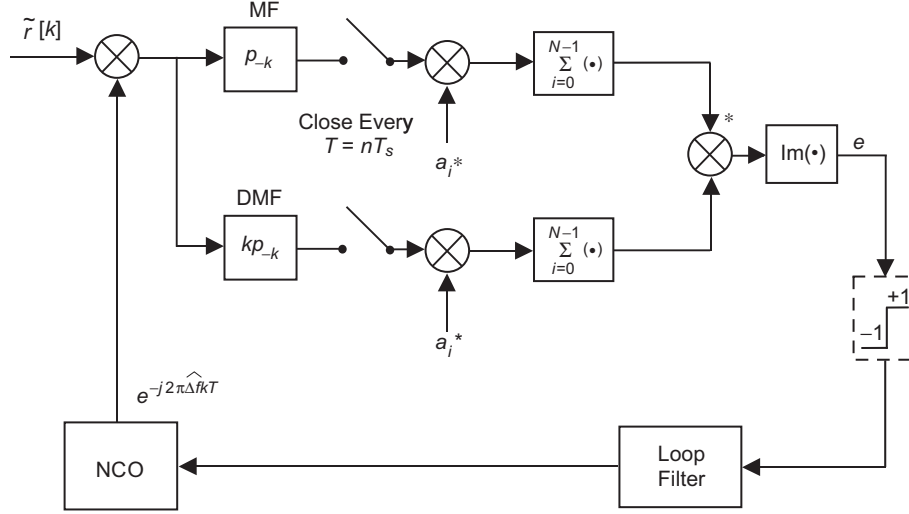


Fig. 4-13. All-digital closed-loop frequency estimator for suppressed carrier, known data.

4.3 Frequency Correction for Modulated Signals with Unknown Data

Consider again a data-modulated signal with no residual (suppressed) carrier. In this section, we assume perfect timing but no knowledge of the data (non-data-aided system). Again using the ML estimation, we derive the open- and closed-loop frequency estimators. In Section 4.2, we obtained the conditional pdf of the received observation given the frequency Δf and data sequence \mathbf{a} . We repeat the result here for clarity:

$$P(\tilde{\mathbf{r}}|\Delta f, \mathbf{a}) = C_8 I_0 \left(\frac{2}{N_0} |Y| \right) \quad (4-45)$$

where

$$Y = \sum_{i=-\infty}^{\infty} a_i^* z_i(\Delta f) \quad (4-46)$$

and

$$z_i(\Delta f) = \int_{iT}^{(i+1)T} \tilde{r}(t) p(t - iT) e^{-j(2\pi\Delta f t)} dt \quad (4-47)$$

Now we have to average Eq. (4-46) over \mathbf{a} . Unfortunately, implementation of this averaging is too complex. Instead, first we approximate the $I_0(x)$ function as

$$I_0\left(\frac{2}{N_0}|Y|\right) \cong 1 + \frac{1}{N_0^2}|Y|^2 \quad (4-48)$$

Now we need only to average $|Y|^2$ over the data sequence \mathbf{a} as

$$\begin{aligned} E\{|Y|^2\} &= E\left\{\left|\sum_{k=0}^{N-1} a_k^* z_k(\Delta f)\right|^2\right\} \\ &= \sum_{k=0}^{N-1} \sum_{i=0}^{N-1} E\{a_k^* a_i\} z_k(\Delta f) z_i^*(\Delta f) \\ &= C_a \sum_{k=0}^{N-1} |z_k(\Delta f)|^2 \end{aligned} \quad (4-49)$$

where $C_a \triangleq E\{|a_k|^2\}$ and the a_k 's are assumed to be zero mean and independent. Thus, estimating the frequency offset over the N data symbol interval can be obtained by maximizing the following metric:

$$\lambda(\Delta f) = \sum_{k=0}^{N-1} |z_k(\Delta f)|^2 \quad (4-50)$$

4.3.1 Open-Loop Frequency Estimation

For open-loop estimation, we have

$$\widehat{\Delta f} = \underset{\Delta f}{\operatorname{argmax}} \lambda(\Delta f) \quad (4-51)$$

However, this operation is equivalent to multiplying the received signal by $e^{-j(2\pi\Delta f t)}$, passing it through a matched filter with impulse response $p(-t)$, and sampling the result at $t = (k+1)T$, which produces the sequence of z_k 's. Next, take the magnitude square of each z_k , perform summation, and then find

the maximum value by varying the frequency Δf between $-\Delta f_{max}$ and Δf_{max} , where Δf_{max} is the maximum expected frequency offset. The block diagram to perform these operations is shown in Fig. 4-14.

4.3.2 Closed-Loop Frequency Estimation

The error signal for closed-loop tracking can be obtained as

$$e = \frac{\partial}{\partial \Delta f} \lambda(\Delta f) \quad (4-52)$$

We can approximate the derivative of $\lambda(\Delta f)$ for small ε as in Eq. (4-17). Then, we can approximate the error signal as

$$e = \sum_{k=0}^{N-1} \{|z_k(\Delta f + \varepsilon)|^2 - |z_k(\Delta f - \varepsilon)|^2\} \quad (4-53)$$

The error signal detector for the closed-loop frequency correction is implemented using the above equations, and it is shown in Fig. 4-15.

Now again, rather than using the approximate derivative of $\lambda(\Delta f)$, we can take the derivative of $\lambda(\Delta f) = \sum_{k=0}^{N-1} |z_k(\Delta f)|^2$ and obtain the error signal as

$$e = \sum_{k=0}^{N-1} \text{Im}\{z_k^*(\Delta f)u_k(\Delta f)\} \quad (4-54)$$

where

$$u_i(\Delta f) = \int_{iT}^{(i+1)T} \tilde{r}(t)tp(t-iT)e^{-j(2\pi\Delta ft)} dt \quad (4-55)$$

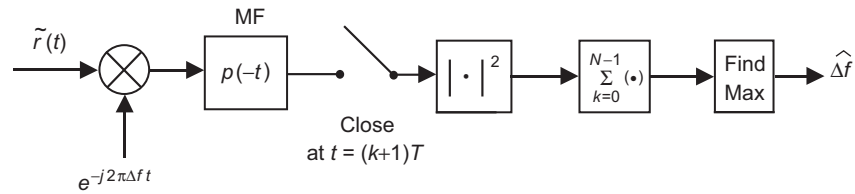


Fig. 4-14. Open-loop frequency estimation for suppressed carrier, unknown data.

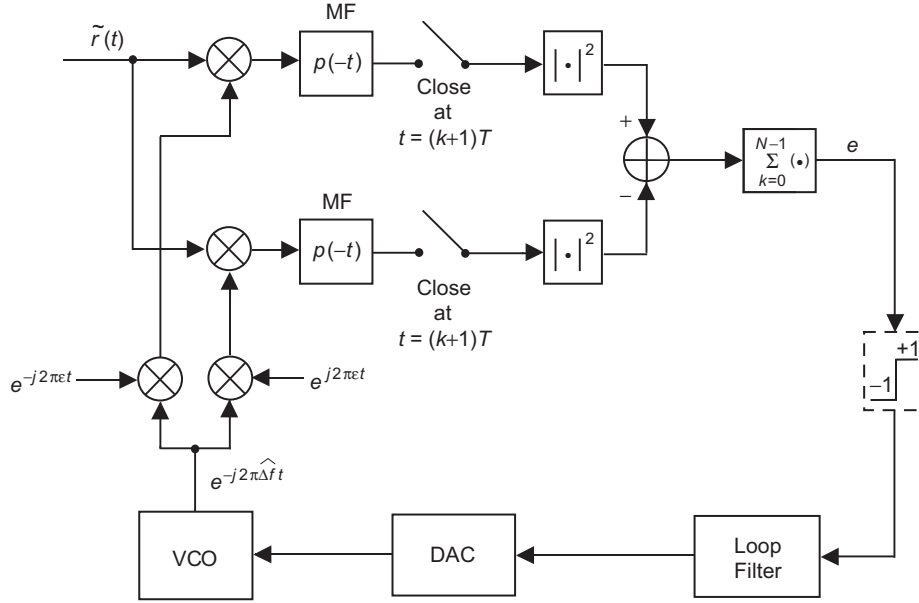


Fig. 4-15. Error signal detector and closed-loop block diagram for suppressed carrier, unknown data.

Note that the error signal in Eq. (4-54) also can be written as

$$e = \sum_{k=0}^{N-1} \{|z_k(\Delta f) - ju_k(\Delta f)|^2 - |z_k(\Delta f) + ju_k(\Delta f)|^2\} \quad (4-56)$$

The block diagram of the closed-loop frequency estimator using the error signal detector given by Eq. (4-54) is shown in Fig. 4-16. Similarly, the block diagram of the closed-loop frequency estimator using the error signal detector given by Eq. (4-56) is shown in Fig. 4-17.

The closed-loop frequency estimator block diagrams shown in this section contain mixed analog and digital circuits. An all-digital version of the closed-loop frequency estimator in Fig. 4-16 operating on the received samples $\tilde{r}[k]$ is shown in Fig. 4-18. All-digital versions of other closed-loop estimators can be obtained similarly.

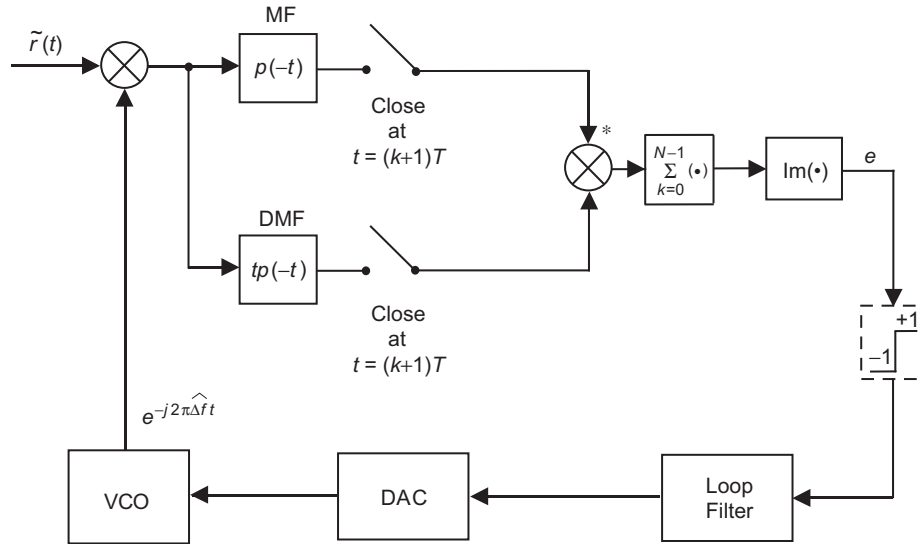


Fig. 4-16. Closed-loop estimator with error signal detector for suppressed carrier, unknown data, Eq. (4-54).

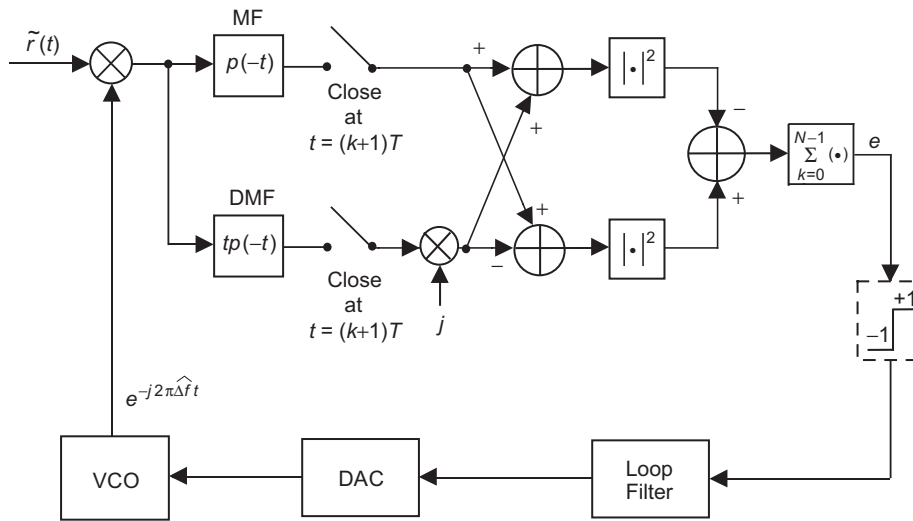


Fig. 4-17. Closed-loop estimator with error signal detector for suppressed carrier, unknown data, Eq. (4-56).

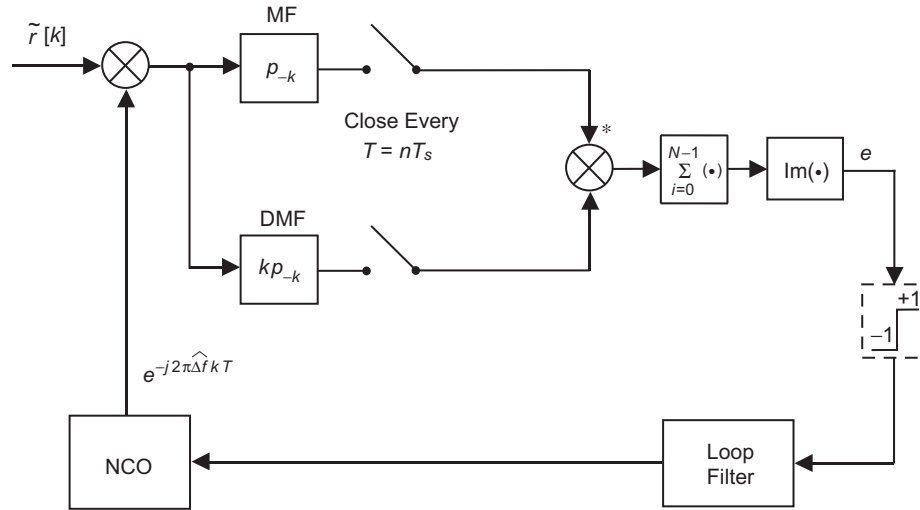


Fig. 4-18. All-digital closed-loop frequency estimator for suppressed carrier, unknown data.

References

- [1] H. Meyr and G. Ascheid, *Synchronization in Digital Communications*, New York: John Wiley and Sons Inc., 1990.
- [2] H. Meyr, M. Moeneclaey, and S. A. Fechtel, *Digital Communication Receivers*, New York: John Wiley and Sons Inc., 1998.